Resistmetric Study of the Potential-sensitive Surface Layer Formed on VO_2 Electrode in a Neutral Solution

Toyohisa NAKAMURA* and Shiro HARUYAMA**

Technical High School, Faculty of Engineering, Tokyo Institute of Technology, 3-3-6, Shibaura, Minato-ku, Tokyo 108

***Faculty of Engineering, Tokyo Institute of Technology, 2-12-1, Ookayama, Meguro-ku, Tokyo 152*

(Received December 27, 1978)

The formation of a potential-dependent surface layer on VO_2 electrode has been investigated from the change in conductance of a thin VO_2 film electrode by galvanostatic polarization. The VO_2 electrode dissolved as vanadate with 100% current efficiency by anodic polarization. At potentials negative to the immersion potential, the VO_2 electrode functioned as an insoluble electrode with the formation of the potential-dependent surface layers of the vanadium oxides by lower valence. The change in composition of the surface layers was traced by resistmetry and coulometry, and illustrated against the amount of electric charge passed, taking V_7O_{13}, V_6O_{11}, V_5O_9, V_4O_7, V_3O_5, and V_2O_3 as the possible oxides. The composition at vanadium oxides of outer-most layer was plotted against the electrode potential. The plot shows a multi-step figure as in the equilibrium partial pressures of oxygen on vanadium oxides at high temperatures, suggesting a model in which the composition of the outer-most layer of the oxide responds to the electrode potential applied.

Resistmetry, a method based on the resistance measurement of a thin film electrode, was first applied to the studies of anodic oxide film on metals by Haruyama and Tsuru[1-4] as an *in-situ* method of measuring the thickness and the electric properties of anodic oxide film.

The potentiostatic transient current on VO_2 electrodes in the cathodic potentials between -0.30 and -1.00 V (SCE) decreases in proportion to the inverse of time asymptotically, the stationary cathodic being below 10^{-5} A/cm^2.[5] In this potential region, the VO_2 electrode functions as an insoluble electrode. A similar behavior has often been observed on transition metals in passive potentials, anodic current flowing in this case.

Iron in passive potentials carries a thin duplex oxide film which consists of an outer γ-Fe_2O_3 and an inner Fe_3O_4 layer.[4-6] It was found by resistmetric studies on passive iron that the structure of the cation-vacant outer-most layer responds to the applied potential.[4] We have applied resistmetry to the thin VO_2 electrode in order to establish the structure of the surface layer formed at the potentials negative to the immersion potential, where the VO_2 electrode works as an insoluble electrode.

Method

When no dissolution process takes place, cathodic polarization of VO_2 electrode yields a thin oxide layer with lower valence on the surface. The conductance of a VO_2 film electrode changes during the course of cathodic reduction. The total conductance of the film electrode is assumed to be the sum of the conductance of the VO_2 substrate and that of the surface layers thus formed. The conductance of each layer is given by

$$K_j = 1/R_j = wt_j/\rho_j l, \tag{1}$$

where t_j and ρ_j are the thickness and the resistivity of j-th layer, respectively, w and l are the width and length of the electrode, respectively. Thus, when a vanadium oxide VO_n is reduced giving VO_{n-x} according to the electrochemical reaction

$$VO_n + 2xH^+ + 2xe^- = VO_{n-x} + xH_2O, \tag{2}$$

the change in conductance Δk_1 during the reduction is given by

$$\Delta k_1 = \frac{W}{2xFl}\left[\frac{M_{n-x}}{\sigma_{n-x}\rho_{n-x}} - \frac{M_n}{\sigma_n\rho_n}\right]Q_1, \tag{3}$$

where M is the molecular weight, ρ the electric resistivity, σ the density, Q the amount of charge passed (C/cm^2), x the number of electron concerned, and suffixes n and $n-x$ represent VO_n and VO_{n-x}, respectively. When the VO_{n-x} formed is reduced to $VO_{n-(x+y)}$,

$$VO_{n-x} + 2yH^+ + 2ye^- = VO_{n-(x+y)} + yH_2O, \tag{4}$$

the change in conductance Δk_2 dealing with Eq. 4 is given by

$$\Delta k_2 = \frac{w}{2yFl}\left[\frac{M_{n-(x+y)}}{\sigma_{n-(x+y)}\rho_{n-(x+y)}} - \frac{M_{n-x}}{\sigma_{n-x}\rho_{n-x}}\right]Q_2, \tag{5}$$

Therefore, the change in conductance Δk ($=\Delta k_1+\Delta k_2$) caused by the reactions of Eqs. 2 and 4 is given by

$$\frac{Q_1}{x}\left[\frac{1}{\rho_{n-x}} - \frac{1}{\rho_n}\right] + \frac{Q_2}{y}\left[\frac{1}{\rho_{n-(x+y)}} - \frac{1}{\rho_{n-x}}\right] = \frac{2Fl\sigma\Delta k}{Mw}, \tag{6}$$

$$Q_1 + Q_2 = Q, \tag{7}$$

where Q represents the total amount of charge passed.

Since the resistivities of vanadium oxides differ a great deal from each other in comparison with the differences in the molecular weight or the density of oxides, the latter differences can be neglected. Thus, we have

$$M \fallingdotseq M_{n-x} \fallingdotseq M_{n-(x+y)} \tag{8}$$

$$\sigma \fallingdotseq \sigma_{n-x} \fallingdotseq \sigma_{n-(x+y)} \tag{9}$$

According to Eqs. 6 and 7, it is possible to separate Q into Q_1 and Q_2 by using the Δk *vs.* Q diagrams and the data of resistivity of oxides. The change in the composition of surface layer of the VO_2 electrode during the course of galvanostatic polarization can be estimated from the k *vs.* time curve and chronopotentiogram. A similar treatment is also possible for the anodic oxidation of the surface layer in a reduced

state.

Experimental

Specimen. The VO_2 film electrode was prepared by the dry oxidation of a vanadium foil. A pure vanadium foil (99.98%) of 0.125 mm thick was oxidized at first in a stream air (1.2 m^3/h) at 873 K for 4 h. The X-ray diffraction pattern of the oxidized surface layer of vanadium shown in Fig. 1-A indicates that the oxidation product consists of V_2O_5, V_6O_{13}, and VO_2. The oxidized vanadium was then reduced in a stream of SO_2 gas (1.2 m^3/h) at 773 K for 2 h. The oxide layer changed to a single phase of VO_2 (Fig. 1-B).[7-8] Since the oxidation process proceeds *via* the vacancy diffusion mechanism, a number of voids should be concentrated at the metal-oxide boundary. The oxide layer can be easily removed from the metallic substrate. In order to prepare the VO_2 film electrode, the oxidized vanadium sample was covered first with an epoxy resin, and then with an acryl resin plate. After the elapse of 12 h for the solidification of the epoxy resin, the VO_2 layer was taken off with the acryl plate from the vanadium substrate. The dimension of the VO_2 electrode thus prepared was 0.015×0.02 m and 10^{-5} m thick. Both ends of the specimen were connected to lead wires by an electric conductive cement and then covered with epoxy resin. The electrode surface was a sort of cleavage surface of black color and moderate brightness.

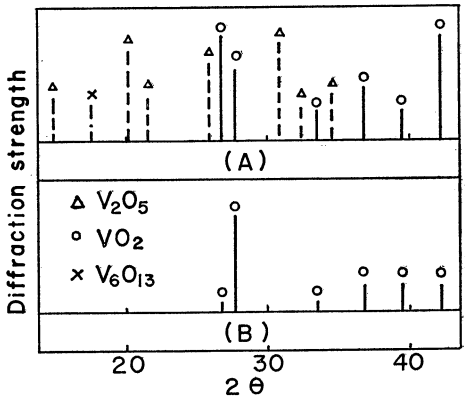

Fig. 1. X-Ray diffraction patterns of vanadium oxides. Preparation of specimen; (A) oxidation of vanadium in air at 873 K for 4 h; (B) reduction of specimen (A) in SO_2 at 773 K for 2 h.

Solution. A mixture of 0.2 mol/l boric acid and 0.05 mol/l sodium borate solution (pH 8.39) was used as an electrolyte solution. Reagent grade chemicals and twice-distilled water were used to prepare the solution. The solution was kept in a storage vessel and deaerated for more than 20 h by bubbling nitrogen gas purified through an active copper bed at 473 K. The solution was transferred from the vessel to the cell or removed from the cell under a nitrogen atmosphere.

Electrical Circuit. The electrical circuit of the resistance measurement is shown in Fig. 2. The change in conductance of the film electrode was traced by recording the unbalanced output voltage of the bridge through a pre-amplifier and a rectifier. The a-c signal between both ends of the film electrode was maintained below 0.005 V in order to minimize an undesirable change in film composition and the by-pass current through the solution. Polarization experiments were carried out with an electronic galvanostat and a counter

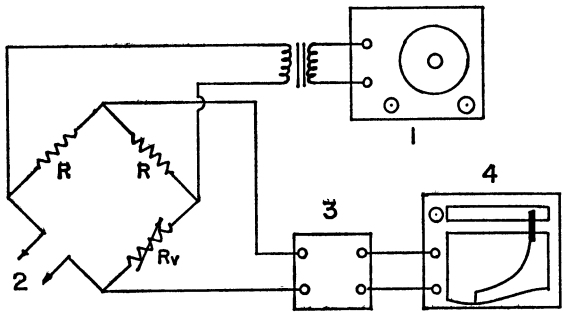

Fig. 2. Diagram of electrical cirucit for conductance measurement.
(1) Oscillator (1 kHz), (2) connected to electrode or standard resistance box, (3) amplifier and rectifier, (4) recorder.

electrode made of a platinum plate. The potential of the film electrode was measured against a saturated calomel electrode *via* a Luggin capillary and a salt bridge. A two-pen recorder was used to record the change in both the potential and the conductance of the film electrode.

Procedure. All the experiments were carried out after anodic treatment at a constant current density of 10^{-5} A/cm^2. After the electrolyte solution had been replaced, the specimen was polarized cathodically at 10^{-5} A/cm^2. The VO_2 electrode did not dissolve except at the final stage of the anodic polarization. The amount of vanadium ion dissolved was analyzed by a colorimetric analysis using the 4-(2-pyridylazo) resorcinol method.[9] The experiments were carried out under a nitrogen atmosphere at 298 K. In order to confirm semiconductive property, the experiment was carried out also under illumination with a 500 W lamp. Illumination effected neither the potential nor the conductance of the film electrode.

Results

Chronopotentiogram of VO_2 Electrode. The VO_2 electrode did not dissolve, functioning as an insoluble electrode at the potentials negative to 0.05 V (SCE) in a solution of pH 8.39.[5] The potentiostatic transient current decreased in proportion to the inverse of time.[5] This indicates the formation of an oxide layer with low valence on the VO_2 electrode, since a similar transient phenomenon is often observed in a film-forming reaction.[6] The VO_2 film electrode was cathodically reduced at first until the potential reached a certain value and then anodically oxidized at a constant current density of 10^{-5} A/cm^2. The chronopotentiograms of the galvanostatic polarization of the VO_2 electrode are shown in Fig. 3. The cathodic polarization of VO_2 electrode was terminated at various potentials, followed by anodic polarization. In the initial periods of cathodic polarization, the potential decreased steeply toward the negative direction to reach E_1, then showing an asymptotic behavior. The chronopotentiogram of the succeeding anodic polarization exhibits two potential arrests E_2 and E_3. Potential E_3 corresponds to a stationary state of the anodic polarization where the anodic dissolution of VO_2 occurred. The amount of electric charge relating to the arrest E_2 increases with the extension of the periods of cathodic polarization.

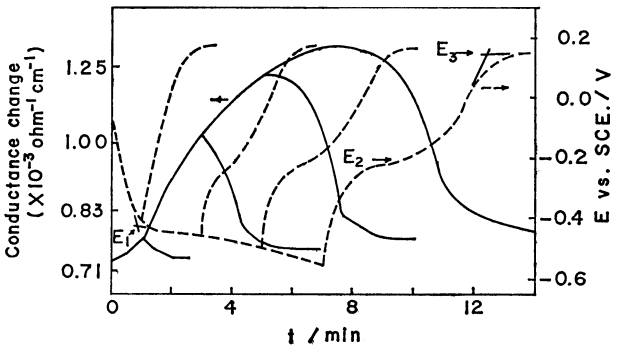

Fig. 3. Change in potential and conductance of VO_2 film during cathodic and anodic polarization at 10^{-5} A/cm².
Solid lines —— conductance change; dashed lines - - potential change.

Anodic Dissolution of VO_2. The VO_2 electrode dissolved at the final stage of anodic polarization. In order to determine the dissolution scheme, the solution after the anodic polarization was examined by colorimetry. The amount of vanadium dissolved and that of the electric charge passed are summarized in Table 1, together with the calculated value of the number of electron in the anodic dissolution of VO_2 electrode. The sample solution for the spectrophotometric analysis was prepared by the anodic dissolution of the VO_2 electrode at a constant current density

Table 1. Number of electrons in the anodic dissolution of VO_2 at 298 K (pH 8.39)

I_a/A cm^{-2} a)	$10^3\,Q_d$/C cm^{-2} b)	$10^6\,W_{s.l.}$/g cm^{-2} c)	N d)
10^{-5}	7.143	3.798	0.993
10^{-5}	9.091	4.833	0.993
5×10^{-5}	7.500	4.026	0.983
5×10^{-5}	5.000	2.607	1.013

a) Current density. b) Amount of anodic charge. c) Weight of vanadium dissolved. d) Number of electrons.

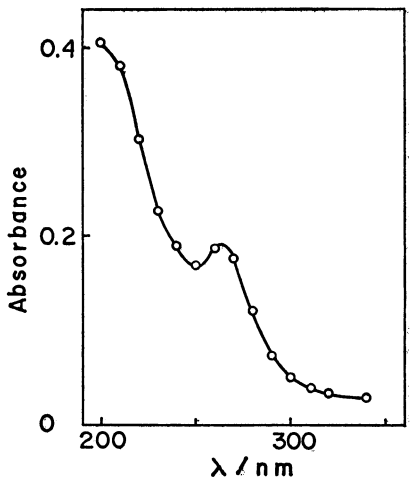

Fig. 4. Absorption spectrum of electrolyte solution after anodic dissolution of VO_2 (4.1×10^{-5} mol/l, pH 8.39).

of 5.0×10^{-5} A/cm² for 21 min. The expected concentration of vanadate(V) was 4.1×10^{-5} mol/l. The absorbance curve of the solution, shown in Fig. 4, is in good agreement with the data of vanadate HVO_4^{2-} reported by Newman *et al.*[10] The anodic dissolution of VO_2 (Fig. 4 and Table 1) proceeds with one electron,

$$VO_2 + 2H_2O = HVO_4^{2-} + 3H^+ + e^-. \quad (10)$$

Change in Conductance on VO_2 Film Electrode During Galvanostatic Polarization. The change in conductance of the VO_2 film electrode during polarization is plotted against the amount of charge passed in Fig. 3, together with corresponding change in potential. In the initial periods of polarization where a steep change in potential is observed, the conductance changes slowly with time. After the potential reaches the arrest E_1, the conductance increases steeply, then exhibiting an asymptotic behavior. The conductance *vs.* time curves of the subsequent anodic polarization are nearly symmetrical to those of the cathodic branch. The conductance of the electrode reverts nearly to the original value at the end of anodic polarization and the electric charge needs to reach the original conductance value increased with extension of the periods of cathodic polarization.

Discussion

Since the VO_2 electrode did not dissolve during the course of polarization at the potentials negative to 0.05 V, the change in conductance (Fig. 3 and Fig. 5-A) is attributed to the formation and the reduction of the oxide layers with different electric resistivity.

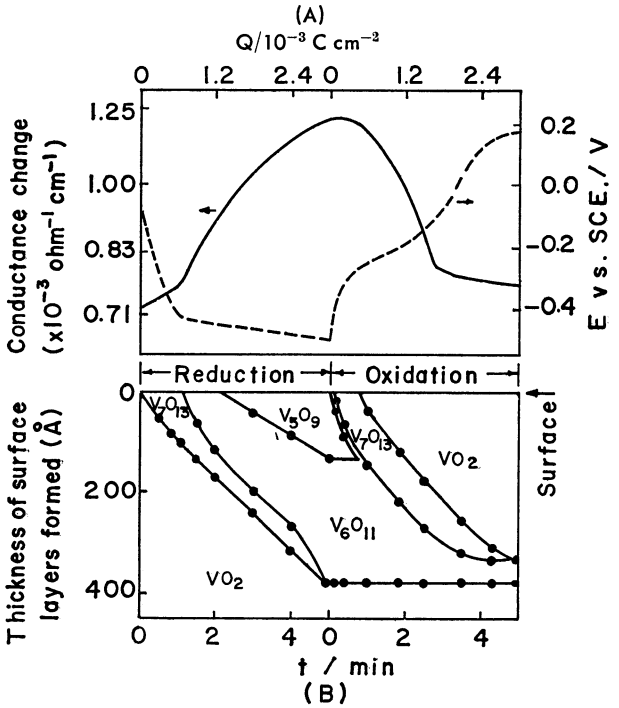

Fig. 5. (A) Change in conductance and potential of VO_2 film during cathodic and anodic polarization curves at 10^{-5} A/cm².
(B) Change in composition of surface layers during cathodic reduction and anodic oxidation of VO_2 film.

TABLE 2. ELECTRIC RESISTIVITY OF VANADIUM OXIDES[11]

Oxide form	Resistivity/Ω cm
VO_2	250
V_7O_{13}	50
V_6O_{11}	4.4
V_5O_9	142
V_4O_7	13.3
V_3O_5	1000
V_2O_3	0.04

In order to estimate the constitution of the surface layers formed by the cathodic polarization, Eqs. 6 and 7 were solved for Q_1 and Q_2, by using the change in conductance and the electric resistivities of vanadium oxides.

The values of resistivity of vanadium oxides show an appreciable scattering. The data given in Table 2[11] were chosen in the following calculation. The thickness of each layer was calculated from Q_1 and Q_2, by means of Eqs. 2 and 4, and the densities of oxides. The species and thicknesses of oxide layers were estimated on the following assumptions.

(1) The VO_2 electrode is reduced in the decreasing order of oxidation state with formation of a multilayer film on surface

$$VO_2 \underset{Q'_1}{\overset{Q_1}{\rightleftharpoons}} V_7O_{13} \underset{Q'_2}{\overset{Q_2}{\rightleftharpoons}} V_6O_{11} \underset{Q'_3}{\overset{Q_3}{\rightleftharpoons}} V_5O_9 \underset{Q'_5}{\overset{Q_4}{\rightleftharpoons}} V_4O_7 \underset{Q'_5}{\overset{Q_5}{\rightleftharpoons}} V_3O_5 \underset{Q'_6}{\overset{Q_6}{\rightleftharpoons}} V_2O_3$$

where Q'_n is the amount of charge concerned with respective reaction.

(2) The thickness of each layer increases or decreases monotonically with time, the total thickness of the surface layers being nearly proportional to the duration of cathodic reduction.

(3) The calculation based on Eqs. 6 and 7 can be applied to the thicknesses of V_7O_{13} and V_6O_{11} in the initial stage of reduction, where only two layers are formed. When the third layer participates in the growth with the progress of reduction, a supplementary procedure is used in the calculation. The growth of the V_7O_{13} layer (Fig. 5-A) follows the following equation in the initial stage of cathodic reduction

$$d = 2.47 \times t^{0.85} \quad (11)$$

where d represents the thickness of the V_7O_{13} layer (Å) and t the time (s). It was assumed that the thickness of the V_7O_{13} layer increases according to Eq. 11 even after the V_5O_9 layer has appeared. The thickness of the V_6O_{11} and V_5O_9 layers was calculated by means of Eqs. 6 and 7 and that of V_5O_9 layer was estimated by Eq. 11.

The results of calculation are illustrated against time in Fig. 5-B. The unit time (1 min) corresponds to 6×10^{-4} C/cm^2, since the polarization experiment was carried out at a constant current density of 10^{-5} A/cm^2. The surface of the VO_2 electrode is seen to be reduced first to V_7O_{13}, and then to V_6O_{11}, which is further reduced to V_5O_9. During the course of

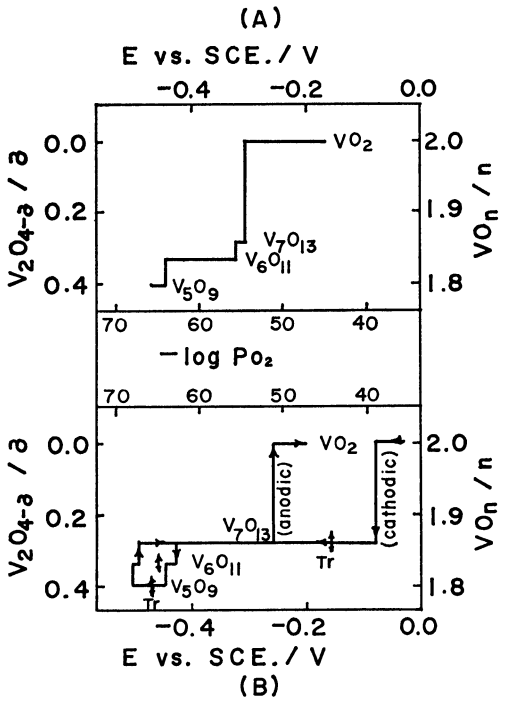

Fig. 6. (A) Relation between vanadium oxides and their eqilibrium pressures of oxygen (from Okinaka's data).
(B) Potential dependency of surface oxides on VO_2 (present work). Tr: Transition potential.

reduction process, the VO_2 substrate is consecutively reduced to the low-valence oxides, the total thickness of the oxide layer increasing in proportion to the amount of electric charge passed. The V_7O_{13} layer vanishes after 5 min of cathodic polarization (3×10^{-3} C/cm^2), the final structure of surface layer consisting of V_5O_9 and V_6O_{11}.

In the subsequent anodic oxidation, V_5O_9 is oxidized to VO_2 *via* V_6O_{11} and V_7O_{13}. Using Fig. 5-B, the oxidation state of the outer-most layer of the VO_2 electrode is plotted against the potential in Fig. 6-B. Since the ohmic drop inside the oxide electrode was estimated to be of the order of 10^{-4} V at the current density chosen, the potential difference should appear mainly at the oxide/electrolyte interface.

The transition from VO_2 to V_7O_{13} occurs at −0.08 V (SCE) in the cathodic process, and at −0.26 V in the anodic process. A similar hysteresis of the transition potential between the cathodic and anodic branch is observed on the transition between V_7O_{13} and V_6O_{11} on that between V_6O_{11} and V_5O_9. Further experiments are necessary to explain, the hysteresis in the transition potential, since it is a sort of underpotential phnomenon.

Thermodynamic properties of vanadium oxides were reported[12-14] mainly from the measurement of the equilibrium partial pressure of oxygen p_{O_2} at high temperature. The composition *vs.* log p_{O_2} diagram of vanadium oxides at 298 K (Fig. 6-A) was estimated by the extrapolation of the data at high temperature to those at 298 K according to the Van't Hoff equation. The log p_{O_2} scale at 298 K was also converted into the potential scale, by considering the Nernst equation

Table 3. Thermodynamic data of vanadium oxides

	Data extrapolated from high temperature measurement (Okinaka *et al.*[12])			Data calculated from transition potential (present work)		
	ΔG°_{298} / kJ mol^{-1}	$-\log p_{O_2}$	E(SCE) pH 8.39	ΔG°_{298} / kJ mol^{-1}	$-\log p_{O_2}$	E(SCE) pH 8.39
VO_2	−658			−658		
		54.6	−0.312		45.1	−0.170
V_7O_{13}	−4447			−4474		
$VO_{13/7}$	−653			−639		
		55.7	−0.328		64.5	−0.465
V_6O_{11}	−3789			−3809		
$VO_{11/6}$	−631			−635		
		64.1	−0.452		67.9	−0.505
V_5O_9	−3127			−3142		
$VO_{9/5}$	−626			−628		

on the reversible potential of oxygen, thus

$$O_2 + 2H_2O + 4e^- = 4OH^- \quad (12)$$

$$E^{rev}_{O_2} = 1.229 + 0.015 \log p_{O_2} - 0.060\ pH \quad (13)$$

Figure 6-A and B are so arranged that the scale of log p_{O_2} and that of potential correspond to each other according to Eq. 13.

Transition potentials and the ($-\log p_{O_2\ 298K}$) at the equilibrium between two oxides are summarized in Table 3, together with the free energy of the formation $\Delta G_{f'298K}$ of the vanadium oxides. The free energy of formation was calculated from ($-\log p_{O_2\ 298K}$) and the transition potentials, assuming that $\Delta G_{f'298K}$ of VO_2 is −314.3 kcal/mol. There is an appreciable disagreement between the values of $\Delta G^\circ_{f'298K}$ calculated from the data of equilibrium partial pressure of oxygen at high temperatures and those from the transition potentials. The former values might be less reliable since they are based on an extended extrapolation from the data at temperatures over 1273 K by using the Van't Hoff equation. On the other hand, uncertainity also exists in the latter method especially on the hysteresis of the transition potentials.

The potential dependency of the surface layer on the VO_2 electrode estimated from the resistmetry (Fig. 5-B) exhibits a quite reasonable behavior as compared with that obtained from the equilibrium partial pressures of oxygen at high temperatures. The results strongly support the model in which the composition of the outer-most layer oxide electrodes changes responding to the applied potential.

The authors wish to thank Prof. Masao Taniguchi, Dr. Tooru Tsuru, and Dr. Masataka Wakihara for their discussions.

References

1) S. Haruyama and T. Tsuru, *Corros. Sci.*, **13**, 275 (1973).
2) T. Tsuru and S. Haruyama, *J. Jpn. Inst. Metals*, **39**, 1098 (1975).
3) T. Tsuru and S. Haruyama, *J. Jpn. Inst. Metals*, **40**, 1172 (1976).
4) S. Haruyama and T. Tsuru, "Passivity and Its Breakdown on Iron and Base Alloys," ed by R. W. Staehle and H. Okada, National Association of Corrosion Engineers, Houston (1976), p. 41.
5) T. Nakamura and S. Haruyama, *Denki Kagaku*, **45**, 309 (1977).
6) M. Nagayama and M. Cohen, *J. Electrochem. Soc.*, **109**, 781 (1962).
7) T. Nakamura, *Report of Technical High School, Faculty of Engineering, Tokyo Institute of Technology*, **8**, 113 (1977).
8) K. Kawashima, K. Kosuge, and S. Kachi, *Chem. Lett.*, **1975**, 1131.
9) Y. Yojou and T. Takeuchi, *Bunseki Kagaku*, **14**, 115 (1965).
10) L. Newman, W. J. Lafleur, J. Brousaides, and A. M. Ross, *J. Am. Chem. Soc.*, **80**, 4491 (1958).
11) S. Kachi, T. Takada, and K. Kosuge, *J. Phys. Soc. Jpn.*, **18**, 1839 (1963).
12) H. Okinaka, K. Kosuge, and S. Kachi, *Trans. Jpn. Inst. Met.*, **12**, 44 (1971).
13) H. Endo, M. Wakihara, M. Taniguchi, and T. Katsura, *Bull. Chem. Soc. Jpn.*, **46**, 2087 (1973).
14) H. Endo, M. Wakihara, and M. Taniguchi, *Chem. Lett.*, **1974** 905.